25th ABCM International Congress of Mechanical Engineering
October 20-25, 2019, Uberlândia, MG, Brazil

CHARPY IMPACT ENERGY CORRELATION WITH FRACTURE TOUGHNESS IN STRUCTURAL STEEL WELDED JOINTS

Kleber E. Bianchi
Federal University of Rio Grande
kleber.bianchi@furg.br

Vitor S. Barbosa
Polytechnic School, University of Sao Paulo
vitor.scarabeli@usp.br

Paulo E. A. Fernandes
National Service for Industrial Training (SENAI-SP)
paulo.fernandes@sp.senai.br

Claudio Ruggieri
Polytechnic School, University of Sao Paulo
claudio.ruggieri@usp.br

Abstract. *An experimental investigation of the cleavage fracture behavior of ASTM A572 Grade 50 steel welds manufactured by different welding processes is reported. The main purpose of the work is the evaluation and discussion on correlations between fracture toughness and Charpy V-notch (CVN) impact energy values for dissimilar materials. Charpy tests at different temperatures were applied in specimens with the notch positioned inside the weld metal, in order to obtain the ductile-to-brittle transition curves. The same procedure was applied in a set of three-point bend specimens, tested to obtain fracture toughness values in terms of the J-integral at cleavage instability,* J_c*. In sequence, the Master Curve approach was applied to obtain an experimentally based value of reference temperature* T_0*, which positions the exponential curve that represents the lower shelf region of the ductile to brittle transition diagram (in terms of fracture toughness instead of CVN data). Finally, this experimentally obtained value of reference temperature,* T_0*, was compared with CVN-based estimates, associated with the impact energy values of 28 J and 41 J, as advocated in crack assessment codes. Obtained results suggest that current correlations need to be adapted to take into account the specific features of each material, particularly in the case of steel welds.*

Keywords: *Fracture toughness, Charpy impact energy, J-integral, Master Curve method, Welded Joints.*

1. INTRODUCTION

Defect assessment procedures currently applied to large engineering structures are based on the balance of fracture toughness and the crack driving force, parameter that represents the stress field intensity in the crack tip and encompasses input data like crack size and loading amplitude. Linear elastic stress intensity factor (K_{Ic}) and elastic-plastic J-integral (J_c) or the Crack Tip Opening Displacement ($CTOD_c$ or simply δ_c) are applied as toughness parameter (Anderson, 2005). Assessment methodologies like BS7910 (2013) and API 579 (2016) directly apply these parameters, which are obtained in laboratory tests on deep crack specimens subjected to a monotonic bending load, in a procedure that ensures a stress-controlled failure by transgranular cleavage mechanism. Such an approach promotes acceptance criteria for cracked structural components and establishes critical flaw sizes for supporting repair decisions and life-extension programs.

Standard codes for fracture evaluation such as ASTM E1820 (2017) and BS 7448 (1991) are currently employed to measure cleavage resistance of structural steels in the ductile to brittle transition curve. However, difficulties still persist in cases where severe limitations exist on material availability, as in older structures for example, where fracture toughness values are usually unknown and cannot be obtained by a test campaign. An alternative is estimating fracture toughness values from simpler and readily available mechanical tests, such as the Charpy V-notch (*CVN*) impact test (Dowling, 1999; ASTM E23-16b, 2016) and, because of that, several studies for obtaining empirical correlations between fracture toughness and Charpy impact energy values were implemented. In a very restrictive procedure, most of these equations associate *CVN* data to the linear elastic K_{Ic} parameter.

Such a conservative approach is indeed necessary, because of remarkable differences in CVN and fracture toughness tests. In a Charpy test, a sudden load is applied over a small, relatively low constrained specimen with a manufactured

V-notch with round tip, whereas in the toughness test, a relatively large specimen with a deep and sharp (fatigue propagated) crack is subjected to a bending (eventually tensile) monotonic load. Consequently, constraint level and stress fields on the fracture region are completely different. So, most of the correlation formulas are applicable only to specific materials, being not able to consider the natural variability promoted by different manufacturing processes and material behaviors.

Recent advances in fitness-for-service (*FFS*) and defect assessment procedures aims to mitigate the undue conservatism associated to the linear elastic approach. These present-day procedures rely on elastic-plastic fracture toughness at cleavage instability, J_c, and its derived parameter K_{Jc}, to characterize the fracture resistance of the material.

Such a scenario evidences the importance of expanding the data set and consequently the applicability of *CVN*-to-fracture toughness correlations. This work addresses an experimental investigation of the cleavage fracture behavior of welded joints, using ASTM A572 Grade 50 steel as base metal, manufactured by different welding processes. Fracture toughness tests conducted on three-point bend *SE(B)* specimens provided the cleavage fracture resistance, J_c, for the weld and base metals. In sequence, the Master Curve approach was applied on the fracture toughness data, providing a reference temperature, T_0, for the tested materials. Conventional Charpy tests allowed characterizing the ductile-to-brittle transition of these materials as well as obtaining temperatures related to specific impact energy values (*28 J* and *41 J*) from which standard based CNV-to-fracture toughness correlations were obtained. The whole set of results allowed to compare the experimentally obtained toughness behavior, in the lower shelf of ductile-to-brittle transition curve, with the one predicted by means of CVN correlations.

2. BASE METAL CHARACTERISTICS AND WELDING PROCEDURES

A hot rolled plate of ASTM A572 Gr.50 steel with thickness of 25.4 mm (1 in) was employed as base metal in the welding procedures. Mechanical strength properties of the plate were 426 MPa and 546 MPa for yield and tensile strength at room temperature. However, fracture toughness and Charpy impact energy data was taken from the work implemented by Barbosa and Ruggieri (2018), which employed test specimens extracted from a plate with thickness of 31.8 mm (1.¼ in). Both test plates presented similar chemical composition and mechanical properties.

Welding of the plates was performed using three widely employed processes: Shielded Metal Arc Welding (*SMAW*), Flux-Cored Arc Welding (*FCAW*) and Submerged Arc Welding (*SAW*). Multi-pass procedures, applied on the flat position, filled the single V-groove joint in order to attain full penetration. All the procedures were performed by skilled welders, with ordinary commercially available materials, devices and accessories. These procedures were prequalified, in accordance with the standard code AWS D1.1/D1.1M (2010).

Filler metal employed in the SMAW process was the AWS A5.1 E7018, a low hydrogen basic coated iron powder electrode, for which the minimum allowable yield strength is 400 MPa and the minimum allowable tensile strength is 482 MPa in the as-welded condition. Welding work steps began by previously drying the 4 mm thick and 450 mm long covered electrodes. A direct current power supply provided a mean value of 185 A and an average voltage of 23 V, which provided an average arc energy of approximately 950 J/mm. Twenty four beads (approximately 2 sticks per each bead) were necessary to completely fill the V groove, including the final pass in the root of the joint after back gouging. The inter-pass temperatures varied between 50ºC and 180ºC. The joint geometry comprised a 30º bevel angle in each plate and, for compensating the contraction of the fused material, a previous angle of 10º between plates was adopted. To mitigate the potential effects of residual stress on the fracture behavior of the weld metal, no mechanical constraint was applied to the plates. The root opening adopted was of 3 mm and the root face was approximately 2.5 mm high.

In the FCAW process, an AWS A5.20 E71T-1M, 1.2 mm thick wire was employed. The standard minimum tensile properties for this wire are the same of the E7018 electrode. The entire coil had been previously dried and maintained in a cabinet until the beginning of the process. A constant voltage power supply provided average voltage of 23V and arc energy of approximately 800 J/mm in the intermediate passes. The shielding gas was a balance of 85% Argon and 15% CO_2. Fourteen beads, applied with a manual torch weaving technique, were necessary to complete the V joint, including the final root pass after gouging. The inter-pass temperatures, as well as the joint geometry, were similar to those applied in the SMAW process.

Finally, the filler metal adopted in the SAW process was a wire AWS EM12K with diameter of 3.2 mm. Average values of current and voltage were 525 A and 30 V, providing an approximate heat input value of 2.5 kJ/mm. The inter-pass temperature was kept lower than 280ºC. Four passes provided completion of the joint, but an additional pass was applied in the root, after a back-gouging process.

3. TENSILE, CHARPY AND TOUGHNESS TESTS FOR EVALUATION OF WELD AND BASE METALS

Mechanical tensile specimens, presenting a diameter of 9 mm in the test section, provided the weld metal stress-strain curve in room temperature. Figure 1(a) shows the positioning of the specimen in relation to the welded joint.

(a) (b)

Figure 1. Relative position of specimen in relation to the weld joint: a) Tensile test and b) CVN

Table 1 summarizes the tensile test results for each welding process. Ultimate to yield strength ratio (σ_{uts}/σ_{ys}) in the range of 1:1 to 1:2 indicates a low hardening behavior of the steel welds, particularly for the FCAW process. For reference, procedure given by Annex F of API 579 (2016) provides the strain hardening exponents, *n*, for the weld metals. An estimate of the yield stress at each test temperature, provided by expression taken from ASTM E1921 (2017), is also presented in the table. Beyond the lower hardening behavior, a high yield strength mismatch between weld and base metals at toughness test temperatures was observed, fact even more accentuated in FCAW case.

Table 1. Tensile test results and derived mechanical properties.

Room temperature					Toughness test temperature		
Material	**Yield σ_{ys} [MPa]**	**Ult$^{\underline{mte}}$ σ_{uts} [MPa]**	σ_{uts}/σ_{ys}	***n***	**Test temp.** (ºC)	**Yield σ_{ysT} [MPa]**	**Mismatch** $\sigma_{ysMSolda}/\sigma_{ysMBase}$
SMAW	519	611	1.2	15	-70	604	1.3
FCAW	576	628	1.1	24	-70	661	1.4
SAW	421	511	1.2	14	-94	543	1.2
Base Metal*	426	543	1.3	11	-20	457	-

* After Barbosa and Ruggieri (2018)

A set of Charpy-V notch (CVN) impact specimens for each welding condition was extracted in the transverse orientation, as shown in Fig 1(b). Impact tests following the requirements of ASTM E23 (2016) were done in a range of temperatures covering the entire interval of ductile-to-brittle behavior transition. The resulting curves are shown in Fig. 2. Results obtained for the base metal by Barbosa and Ruggieri (2018) were also inserted in the figure. The symbols represent the experimental data and the lines define the hyperbolic tangent curve fitting, after EricksonKirk et al. (2008).

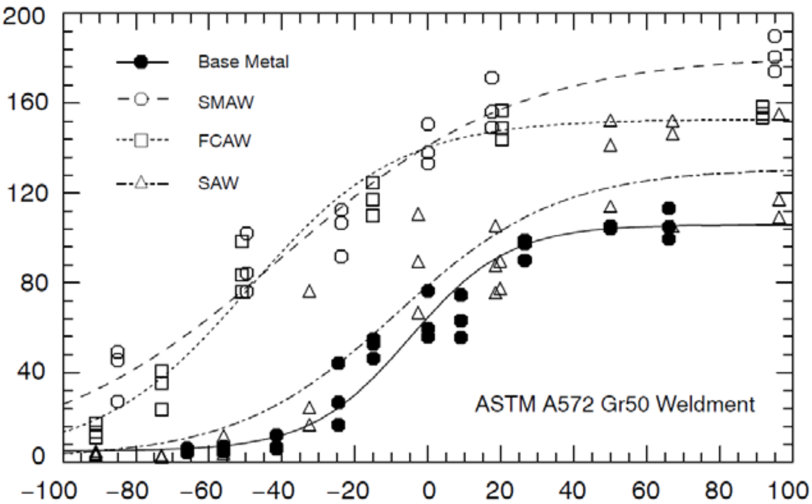

Figure 2. Ductile to brittle transition curves based on Charpy test results (CVN *vs*. temperature).

The fitting equations allowed obtaining the transition temperatures corresponding to 28 J and 41 J impact energies, which are shown in Tab. 2. These auxiliary temperatures will be employed for obtaining estimates of the reference temperature, T_0, as explained in the following section.

Table 2. Temperature values associated to impact energies of 28 J (T_{CVN28}) and 41 J (T_{CVN41}).

Material	**T at 28 J**	**T at 41 J**
SMAW	-97 ºC	-81 ºC
FCAW	-81 ºC	-71 ºC
SAW	-39 ºC	-27 ºC
Base Metal	-22 ºC	-13 ºC

Fracture toughness tests were performed in accordance with ASTM E1820 (2017) and ASTM E1921 (2017) on conventional, plane-sided three-point bend specimens with a square section (*B=W=20 mm*). Position of the specimen in relation to the welded joint is shown in Fig.3. The notch was manufactured in the weld centerline and a previously fatigue-generated crack with length-to-width ratio (*a/W*) equal to 0.5 provided the constraint conditions necessary for predominance of a cleavage fracture process. Finally, a load span of 80 mm was adopted.

In order to measure the *J*-integral values at cleavage instability (J_c), SMAW and FCAW weld metals had been tested in a temperature of –70ºC, while the SAW case demanded an even lower temperature, of –94ºC. These temperatures surely correspond to the lower-shelf region of the ductile-to-brittle transition curve.

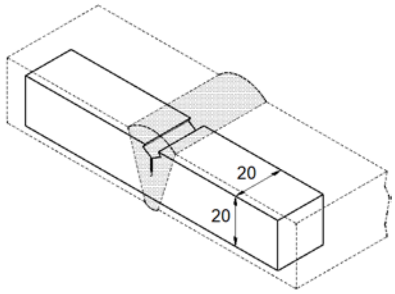

Figure 3. Relative position of fracture toughness SE(B) specimen.

For each specimen, measurements of Load *vs.* CMOD (Crack Mouth Opening Displacement) were obtained and stored. The CMOD signal was originated by a clip gauge, mounted over a knife-edge groove machined on the notch mouth. All Load *vs.* CMOD data where analyzed in the software FRACTUS (Ruggieri, 2011) for obtaining linear elastic and plastic parameters, as well as the onset point of cleavage fracture. All obtained curves for the analyzed weld metals presented a superior area, and consequently propitiated higher toughness values, in comparison with the base metal data provided by Barbosa and Ruggieri (2018). Post-mortem examination of the fracture surfaces revealed essentially no ductile tearing prior to cleavage fracture for the specimens in all welding conditions, which provided strong support to the master curve analysis. Figure 4 shows a scanning electron microscope image of the resulting fracture surface of a FCAW specimen. The region analyzed corresponds to the center of the specimen, near to the tip of the original fatigue-generated crack. The others weld metal cases presented similar behavior.

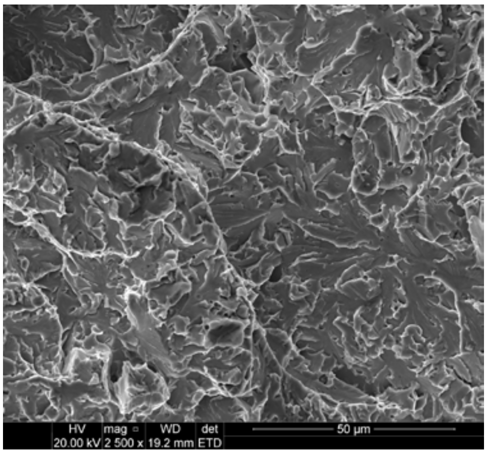

Figure 4. Image of the fracture surface of FCAW weld metal.

Measured values of J_c were inside an interval of *32-240 kJ/m²* for *SMAW*, *20-201 kJ/m²* for *FCAW*, *40-99 kJ/m²* for *SAW* weld metals. Base metal results (Barbosa and Ruggieri, 2018) were spread in an interval of *27* and *47 kJ/m²*. The results outline that the higher fracture toughness values presented by the weld metals in respect to base material are also accompanied by a remarkable scatter. Finally, no clear trend related to mismatch effect was observed.

4. MASTER CURVE ANALYSIS

The Master Curve is a statistically based methodology that adopts an index parameter known as the reference temperature (T_0), which positions the fracture toughness *vs.* temperature relation corresponding to the lower shelf of the brittle-to-ductile transition curve. In such a region, a cleavage fracture mechanism strongly prevails, with no previous tearing or perceptible crack tip plasticity. ASTM E1921 (2017) contains several analytical and experimental aspects related to the methodology. For a deeper review, please refer to the work by Wallin (1984), among others.

The approach begins by a convenient conversion of the *J*-integral at cleavage instability values (J_c) into an equivalent parameter K_{Jc} ($K_{Jc} = [EJ_c/(1-\nu^2)]^{1/2}$. The reference parameter T_0 is, by definition, the temperature in which the equivalent toughness value (K_{Jc}) is equal to 100 MPa(m)$^{1/2}$, in a 1T specimen ($B = 1\ in \approx 25\ mm$). Such a parameter is obtained by a set of single or multi-temperature toughness tests, in which a relatively small quantity of specimens is usually necessary.

After obtaining the reference temperature value, the median K_{Jc} *vs* temperature curve is plotted by applying Eq. (1):

$$K_{Jc(median)} = 30 + 70e^{[0.019(T-T_0)]} \tag{1}$$

The method also includes equations for correction of toughness values in case of specimens with different thickness than the standard (*1T*) dimension. Additionally, provides the possibility of drawing tolerance bounds, derived from the original median curve.

Following this brief introduction of the master curve methodology, the corresponding attained results can be presented. After conclusion of toughness tests, the single-temperature methodology prescribed by ASTM E1921 (2017) was applied to obtain the reference temperature T_0. As yet explained, the J_c toughness values were primarily converted in equivalent K_{Jc} and corrected to consider the right thickness, because weld metal specimens presented $B = 20\ mm$ (*0.8T*). Such a correction was not necessary for the toughness data reported by Barbosa and Ruggieri (2018).

Table 3 presents the final equivalent toughness values obtained for the base metal (9 specimens) and for the weld metals (7 specimens per each welding process).

Table 3. Corrected (1T) equivalent toughness values.

Corrected K_{Jc} values [MPa(m)$^{1/2}$]			
Base Metal*	**SMAW**	**FCAW**	**SAW**
79	85.1	68.8	101.6
97.5	108.3	80.8	103.1
101	134.1	92.7	131.1
103.2	143	95.9	139.4
117.4	176.2	119.3	141.8
119.9	186	131.7	153.4
122	210.2 (**229 .7**)	217.7	159.9
131.6	-	-	-
134.5	-	-	-

* as reported by Barbosa and Ruggieri (2018)

One of the SMAW specimens achieved an equivalent fracture toughness value that, in accordance with ASTM E1921, should be censured, because such a value was greater than the proper capacity of the specimen. So, the toughness corresponding to 229.7 MPa(m)$^{1/2}$, highlighted with bold letters in the table, was replaced by the limit value obtained by Eq. (2):

$$K_{Jc(limit)} = \sqrt{\frac{Eb_0\sigma_{ys}}{30(1-\nu^2)}} \tag{2}$$

In which: E is the Young modulus, b_0 is the remaining ligament, σ_{ys} corresponds to yield strength and ν is the Poisson Ratio.

The Master Curve can be viewed as a fitting method based in a Weibull distribution. The master curve scale parameter (K_o) is obtained by Eq. (3):

$$K_0 = 20 + \sqrt[4]{\left[\sum_{i=1}^{N} \frac{(K_{Jc(i)} - 20)^4}{r}\right]} \tag{3}$$

in which r corresponds to the number of uncensored data and N is the total number of uncensored and censored data.

The K_{Jc} median value of a group of fractured specimens is obtained by means of Eq. (4):

$$K_{Jc(med)} = 20 + (K_0 - 20)\sqrt[4]{\ln(2)} \tag{4}$$

Finally, the first estimative of T_0 is obtained by means of Eq. (5):

$$T_{0Q} = T - \left(\frac{1}{0.019}\right)\ln\left[\frac{(K_{Jc(med)} - 30)}{70}\right] \tag{5}$$

in which, T [^oC] is the test temperature adopted for the group of specimens.

The preliminary estimate is confirmed after verifying if all preconized requirements of the method had been accomplished. Such a set of requirements ensures the constraint level and stress triaxility at crack tip that effectively conduct to the predominance of a cleavage fracture process in the specimens. All these requirements were attained in the tests and, as a result, estimates were naturally converted in effective T_0 values. These values are shown in Tab. 4.

Table 4. Final T_0 values attained by the single test temperature method of ASTM E1921.

Single-temperature toughness tests			
Base Metal	**SMAW**	**FCAW**	**SAW**
-26ºC	-102ºC	-92ºC	-111ºC

Figure 5 provides the master curves obtained by applying the attained reference temperatures in Eq. (1). These diagrams represent the variation of K_{Jc} with temperature for the tested base and weld metals. Solid lines define the median master curve whereas dashed lines represent the 5% and 95% tolerance bounds. The measured K_{Jc}-values are included in the plot. Examination of these results clearly reveals a marked decrease in the reference temperature for the weld metals in comparison with T_0-value of the base metal. It is also possible to observe that the tolerance bounds do not envelope all measured toughness values for the SMAW and FCAW welding processes, which is an additional evidence of the large scatter of results.

5. CVN-BASED REFERENCE TEMPERATURE ESTIMATES

The ASTM E1921 code also provides correlations between T_0 and the temperatures corresponding to the impact energy values of *28 J* and *41 J* (T_{CVN28} and T_{CVN41}), attained in a CVN-based ductile-to-brittle transition curve. These correlations are described by Eq. (6):

$$\begin{aligned} \overline{T}_{0_{28}} &= T_{CVN28} - 18^oC \\ \overline{T}_{0_{41}} &= T_{CVN41} - 26^oC \end{aligned} \tag{6}$$

The fitting procedure adopted to plot Fig. 2 allowed to obtain the temperatures T_{CVN28} and T_{CVN41} that, after had been applied in Eq.(6), generated the estimates presented in Tab. 5 (the T_0 values presented in Tab.4 were repeated to facilitate comparison of results).

Table 5. Estimated T_0-values (ºC) obtained by empirical correlations and by master curve method.

Material	**CVN-based estimates**		**Master Curve Method (ºC)**
	T_{CVN28}-18 (ºC)	**T_{CVN41}-24 (ºC)**	
SMAW	-115 *	-107 *	-102
FCAW	-99 *	-97 *	-92
SAW	-57	-53	-111
Base Metal	-40 *	-39 *	-26

* Non-conservative value, albeit inside the +/-15ºC interval preconized by ASTM E1921 code.

In both SMAW and FCAW cases, the estimated T_0 is consistently lower, which is a non-conservative and undesirable result. However the relatively small differences between estimates and the Master Curve-based reference temperature are inside the interval preconized by the proper ASTM E1921 code. In particular, the predicted T_0 for the FCAW process is in relatively good agreement with the master curve analysis. A similar trend is also observed for the base material.

For the SAW case instead, the estimated T_0 values, whatever the equation considered, are substantially higher in relation to that obtained in master curve approach.

In a summary, the predicted T_0-values (specially for SAW case) display unexpected and important differences.

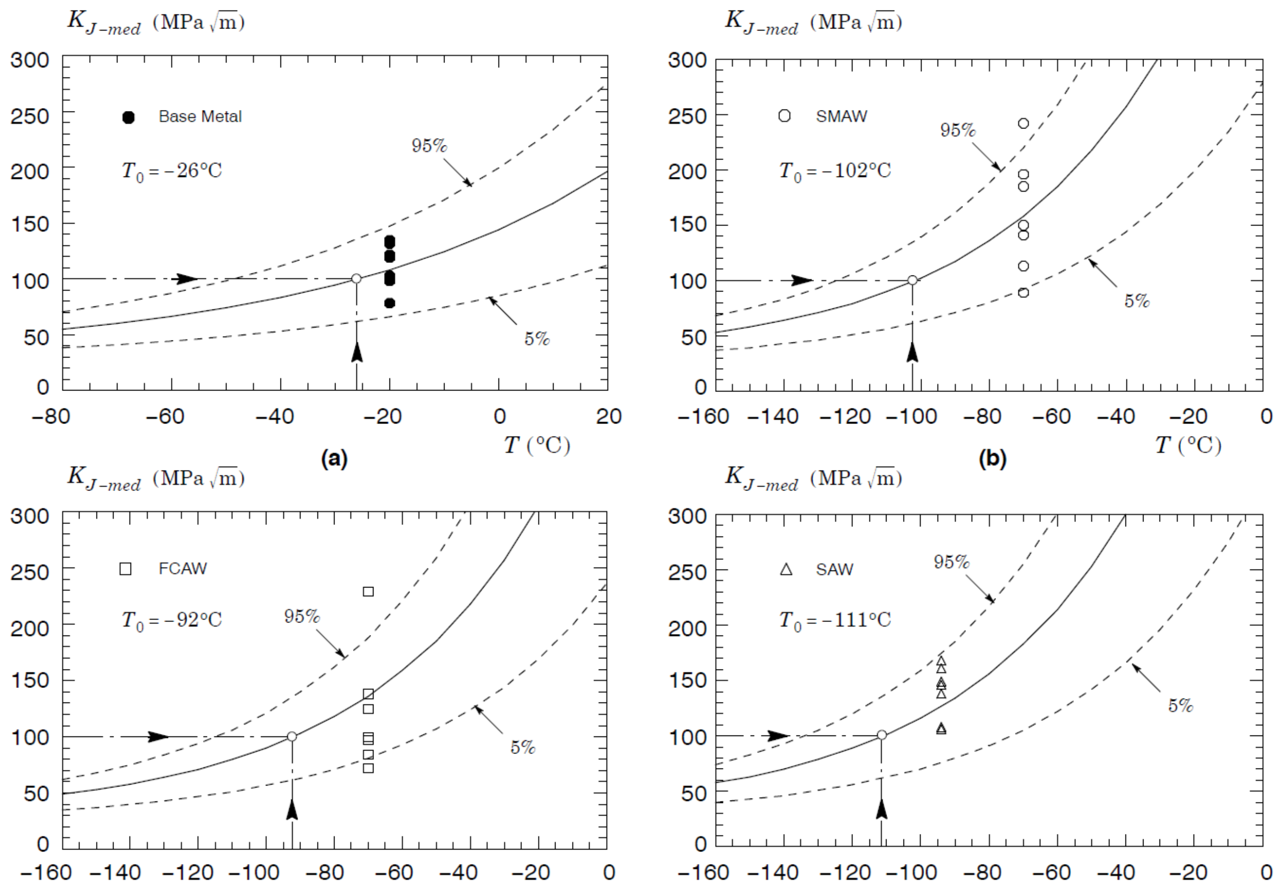

Figure 5. Master curves obtained from the measured fracture toughness tests: a) base metal, b) SMAW weld metal, c) FCAW weld metal and d) SAW weld metal.

6. CONCLUDING REMARKS

Reported results indicate that CVN-to-fracture toughness correlations for SMAW and FCAW weld metals provide a non-conservative assessment for flawed structural components. Similar trends are also observed in the case of the correlation between CVN energy and fracture toughness for the ASTM A572 Grade 50 base material tested by Barbosa and Ruggieri (2018). However, in the SAW case the correlation propitiated predicted toughness values which are higher than the corresponding experimentally measured values. The opposed observed trends indicate that current CVN-to-fracture toughness correlations need to be expanded in order to take into account the specific features of each material, particularly in the case of steel welds.

7. REFERENCES

Anderson, T. L., 2005. “Fracture Mechanics: Fundaments and Applications” - 3rd ed, CRC Press, Boca Raton, USA.

API RP-579-1 / ASME FFS-1, 2016. “Fitness-for-service”, American Petroleum Institute.

ASTM E1820, 2017. “Standard test method for measurement of fracture toughness”, American Society for Testing and Materials, West Conshohocken, PA, USA.

ASTM E1921-17a, 2017. “Standard test method for determination of reference temperature, T0, for ferritic steels in the transition range”, American Society for Testing and Materials, West Conshohocken, PA, USA.

ASTM E23-16b, 2016. “Standard test method for notched bar impact testing of metallic materials”, American Society for Testing and Materials, West Conshohocken, USA.

AWS (American Welding Society), 2010. Structural Welding Code – Steel. D1.1/D1.1M.

Barbosa, V. S. and Ruggieri, C., 2018. "Fracture toughness testing using non-standard bend specimens - Part II: Experiments and evaluation of t0 reference temperature for a low alloy structural steel", Engineering Fracture Mechanics 195 (2018) 297–312.

BS 7448-1, 1997. "Fracture mechanics toughness tests - Part 1. Method for determination of KIc, critical CTOD and critical J values of metallic materials", British Standards Institution, London, UK.

BS 7910, 2013. "Guide to methods for assessing the acceptability of flaws in metallic structures", British Standard Institution, London, UK.

Dowling, N. E., 1999. "Mechanical Behavior of Materials: Engineering Methods for Deformation, Fracture and Fatigue", 2nd Edition, Prentice Hall, New Jersey, USA.

EricksonKirk, M. T., Shaikh, A., EricksonKirk, M.A., 2008. "Insights and observations arising from curve-fitting the Charpy V-notch and tensile data contained within the United States LightWater reactor surveillance database", in: ASME PVP 2008, American Society of Mechanical Engineers, Chicago, USA.

Ruggieri, C., 2011, "FRACTUS2D: numerical computation of fracture mechanics parameters for 2-D cracked solids". Tech. rep., University of Sao Paulo.

Wallin, K., 1984. "The scatter in KIc results", Engineering Fracture Mechanics 19 (1984) 1085–1093. Responsibility notice The authors are the only responsible for the printed material included in this paper.

8. RESPONSIBILITY NOTICE

The authors are the only responsible for the printed material included in this paper.